

## Measuring airway exchange of endogenous acetone using a single-exhalation breathing maneuver

Joseph C. Anderson,<sup>1</sup> Wayne J. E. Lamm,<sup>1</sup> and Michael P. Hlastala<sup>1,2</sup>

Departments of <sup>1</sup>Medicine and <sup>2</sup>Physiology and Biophysics, University of Washington, Seattle, Washington

Submitted 18 July 2005; accepted in final form 2 November 2005

**Anderson, Joseph C., Wayne J. E. Lamm, and Michael P. Hlastala.** Measuring airway exchange of endogenous acetone using a single-exhalation breathing maneuver. *J Appl Physiol* 100: 880–889, 2006. First published November 10, 2005; doi:10.1152/jappphysiol.00868.2005.—Exhaled acetone is measured to estimate exposure or monitor diabetes and congestive heart failure. Interpreting this measurement depends critically on where acetone exchanges in the lung. Health professionals assume exhaled acetone originates from alveolar gas exchange, but experimental data and theoretical predictions suggest that acetone comes predominantly from airway gas exchange. We measured endogenous acetone in the exhaled breath to evaluate acetone exchange in the lung. The acetone concentration in the exhalate of healthy human subjects was measured dynamically with a quadrupole mass spectrometer and was plotted against exhaled volume. Each subject performed a series of breathing maneuvers in which the steady exhaled flow rate was the only variable. Acetone phase III had a positive slope ( $0.054 \pm 0.016 \text{ liter}^{-1}$ ) that was statistically independent of flow rate. Exhaled acetone concentration was normalized by acetone concentration in the alveolar air, as estimated by isothermal rebreathing. Acetone concentration in the rebreathed breath ranged from 0.8 to 2.0 parts per million. Normalized end-exhaled acetone concentration was dependent on flow and was  $0.79 \pm 0.04$  and  $0.85 \pm 0.04$  for the slow and fast exhalation rates, respectively. A mathematical model of airway and alveolar gas exchange was used to evaluate acetone transport in the lung. By doubling the connective tissue (epithelium + mucosal tissue) thickness, this model predicted accurately ( $R^2 = 0.94 \pm 0.05$ ) the experimentally measured expirograms and demonstrated that most acetone exchange occurred in the airways of the lung. Therefore, assays using exhaled acetone measurements need to be reevaluated because they may underestimate blood levels.

mathematical model; isothermal rebreathing; gas exchange; breath test; mass spectrometer

SAMPLING EXHALED BREATH IS a common procedure in many professions to determine medical or legal status. Respiratory therapists measure end-exhaled carbon dioxide to determine gas exchange efficiency of the lung. Industrial hygienists use a breath sample to estimate a worker's exposure to chemical solvents such as toluene and acetone. Toxicologists and police officers rely on the single-breath test to estimate blood alcohol content in workers and automobile drivers. More recently, clinical investigators have begun to sample the end-exhaled breath for endogenous gases such as ethane, propane, isoprene, and acetone that may be markers of common disorders such as lung cancer (31), acute myocardial infarction (23), and congestive heart failure (21).

Because of its close association with the ketogenic state, many investigators have measured endogenous acetone in the exhaled breath and correlated this concentration to clinical outcomes. One study used breath acetone to estimate the

ketotic state during fasting (36) and the metabolic state in newborn babies (28). Breath acetone has been studied as a tool to examine the relationship between ketogenic diets and seizure control (26, 27). Additionally, subjects on a restricted-calorie weight-loss program have used breath acetone as a motivational tool and measure of the program's effectiveness (20). Another team of investigators reported elevated breath acetone levels during congestive heart failure (21). Other researchers have suggested that breath acetone was more effective than urine samples for monitoring ketonemia in insulin-dependent diabetic patients with high ketone levels (20). Recently, the analysis of breath acetone and ethanol, both of endogenous origin, has been used to approximate the blood glucose level during a glucose load (10).

Although these studies examine a variety of clinical outcomes, these studies have two common features: endogenous acetone and, more importantly, the breath test. A breath test requires a subject to inspire fresh air and expire into a collection container or measuring device. Many studies required subjects to take a tidal breath (25, 27, 36). In other studies, investigators asked subjects to perform a prolonged expiration: inspire to total lung capacity (TLC) and expire slowly to residual volume (10, 21). Although different breathing maneuvers were used among studies, the investigators appeared to share two assumptions on collecting an exhaled gas sample. When collecting exhaled breath, most investigators discarded the first portion of the breath, assuming it is "dead space air" that has not contributed to gas exchange, and sampled the final part of the exhalation, assuming that it represents alveolar air (10, 21, 25, 27, 36). While these assumptions are standard for carbon dioxide exchange in the lung, no studies have demonstrated that these assumptions are correct for acetone exchange.

In the present study, we investigated endogenous acetone exchange in the lungs of healthy humans during a prolonged exhalation maneuver. The primary purpose was to determine whether acetone exchanges in the airways, as suggested by experimental and theoretical studies (1, 19, 34, 35). If the airways act as an exchange space, we hypothesized that the dead space calculated using an exhaled acetone profile would be small or nonexistent and the end-exhaled gas concentration would be less than the alveolar gas concentration. The alveolar gas concentration was estimated with an isothermal rebreathing maneuver, similar to the technique used by Ohlsson et al. (29) and Martin (22). A secondary goal of this investigation was to further validate a mathematical model of airway and alveolar gas exchange (1). This mathematical model, developed in this laboratory, describes the simultaneous exchange of heat, water,

Address for reprint requests and other correspondence: J. C. Anderson, Division of Pulmonary and Critical Care Medicine, Box 356522, Univ. of Washington, Seattle, Washington 98195–6522 (e-mail: clarkja@u.washington.edu).

The costs of publication of this article were defrayed in part by the payment of page charges. The article must therefore be hereby marked "advertisement" in accordance with 18 U.S.C. Section 1734 solely to indicate this fact.

and a soluble gas with the airways and alveoli. Once validated, the model simulations were examined to explain the mechanisms of acetone exchange in the lungs. A tertiary and minor aim of this study was to provide an understanding of the physical mechanisms of acetone exchange, which would form a foundation to develop a standard protocol for collecting endogenous acetone in the exhaled breath that is representative of the alveolar gas.

## METHODS

### Mathematical Model

A detailed description of the model has been published previously (1). Only the essential features will be described here. The model has a symmetric bifurcating structure through 18 generations. The dimensions of the airways for the upper respiratory tract are from Hanna and Scherer (14), and those for the lower respiratory tract are from Weibel (40). The upper respiratory tract and intraparenchymal airways are divided into 480 axial control volumes. Radially, the airways are divided into six layers: 1) the airway lumen, 2) a thin mucous layer, 3) connective tissue (epithelium and mucosal tissue), 4) the bronchial circulation, 5) the adventitia, and 6) the pulmonary circulation. Cartilaginous airways (generation < 10) functionally, only have the first four layers. Within a control volume, the surface area for exchange between radial layers is assumed to be constant and equal to  $\pi d \Delta z$ , where  $d$  is the diameter of the airway lumen and  $\Delta z$  is the axial length of the control volume. The respiratory bronchioles and alveoli are lumped together into a single alveolar unit. The concentration of soluble gas in the alveolar air is allowed to vary with time and depends on the pulmonary blood flow, ventilation, blood solubility, and concentration of soluble gas in the incoming blood, as described by a mass balance on the alveolar compartment.

Within each radial layer, concentration and temperature values are bulk averages for the entire layer. The air in the lumen is considered a mixture of dry air, water vapor, and a single soluble gas (e.g., acetone). Mass and energy are transported between control volumes by bulk convection and axial diffusion through the lumen. Radial transport between the gas phase and mucous layer is described with heat and mass transfer coefficients that are determined from empirical correlations (6, 17). Near the air-mucus interface, local vapor-liquid equilibrium is described by Raoult's law for water and the water-air partition coefficient for the soluble gas. The mucous layer is assumed to have the properties of water and can change thickness, depending on local hydration and dehydration. A minimum mucous layer thickness is maintained by filtration of water from the bronchial circulation through the connective tissue layer and into the mucous layer. Transport of water and soluble gas between these three layers occurs via filtration and diffusion (Fick's law). The connective tissue layer and the adventitial tissue layer are treated as a binary mixture of dilute soluble gas and water. The diffusivity of a soluble gas through the connective and adventitial tissue is assumed to be 33% of its diffusivity in water. For a soluble gas, the tissue solubility is assumed to be equal to blood solubility. The dimensions of the connective tissue, bronchial circulation, and adventitial tissue layers (i.e., radial thickness, surface area, and cross-sectional area) are calculated by scaling measurements made in sheep (2) to those of a human (1). The bronchial circulation is modeled as an axial series of annular sheets of blood interposed between the connective and adventitial tissue layers. Blood enters the control volume at body temperature, and with a systemic concentration of soluble gas, exchanges energy and mass via filtration and diffusion with the surrounding tissue, and leaves the control volume at a venous temperature and soluble gas concentration. Adjacent to the adventitial tissue layer, the pulmonary capillary bed is assumed to be at body temperature, and the concentration of soluble gas is assumed to be the average of the soluble gas concentration entering and leaving the alveolar unit via the pulmonary circulation.

The concentration of soluble gas in the venous blood entering the pulmonary circulation is specified. The systemic concentration of soluble gas is calculated by solving the equation describing mass accumulation in the alveolar compartment.

Mass and energy balances around a control volume produce 3 partial- and 9 ordinary-differential equations in time,  $t$ , and space,  $z$ . The equations are solved simultaneously for the following 12 dependent variables: the mole fraction of soluble gas in the air, mucous, connective tissue, bronchial bed, and adventitial tissue layers; the temperature of the air, mucous, connective tissue, bronchial bed, and adventitial tissue layers; the mole fraction of water in the air; and the mucous thickness. The 12 differential equations are solved numerically on a Pentium IV computer running DIGITAL Visual Fortran. The spatial derivatives are solved by upwind finite difference, while the time derivatives are handled using LSODE, an integrating software package developed by Hindmarsh (16). The mass balance around the alveolar compartment is integrated separately from the airway control volumes using LSODE.

### Experimental Measurements

**Subjects.** The eight healthy subjects (4 men and 4 women) used in this study had the following (mean  $\pm$  SD) characteristics: age  $35 \pm 10$  yr and height  $171 \pm 7$  cm. Characteristics of the subjects are summarized in Table 1. Subjects were included in this study, if their responses to a medical questionnaire indicated that they had not smoked within the past 3 yr; had no history of asthma, chronic respiratory disease, or cardiac diseases; and did not participate in an activity that predisposed them to chemical solvents. The Institutional Review Board at the University of Washington approved the protocol, and written, informed consent was obtained from each subject.

**Mass spectrometer.** Acetone concentration in the exhaled breath was measured with a quadrupole mass spectrometer (Balzers Omnistar, Balzers, Liechtenstein) by monitoring the peak at the mass-to-charge ratio of 58. With tuning, the instrument can measure 0.25 parts per million (ppm) levels of acetone with a signal-to-noise ratio of 3. The transit delay time is 450 ms, and the 0–90% response time is 400 ms. The mass spectrometer sampled the airstream at a rate of 7.5 ml/min through a heated inlet maintained at 100°C. The instrument was calibrated with a known concentration of acetone (serially diluted to  $\sim 1.5$  ppm) every 15 min throughout the experiment enabling off-line correction of signal drift from the instrument. Based on the calibration measurements, the average ( $\pm$ SD) drift of the mass spectrometer signal from the eight experiments was  $0.06 \pm 0.15$  ppm/h. The rate of drift was constant over the course of each 2-h experiment.

**Prolonged exhalation measurements.** The mouthpiece assembly consisted of a disposable mouthpiece with two small ports drilled into the bottom, allowing the inlet of the mass spectrometer and a thermocouple (K-type, 0.002 in. in diameter, Omega Engineering, Stamford, CT) to be locked into place and positioned  $\sim 2$  and 2.5 cm from the subject's lips, respectively. Attached to the distal end of the mouthpiece were the following in sequential order: a pneumotach (RSS 100, Korr Medical Technologies, Salt Lake, UT), a capnometer

Table 1. Subject characteristics

Subject No.	Gender	Age, yr	Height, cm	Weight, kg	MEV, ml
1	M	53	178	65	4,700
2	M	32	183	75	4,700
3	M	41	170	91	3,300
4	M	41	170	68	4,100
5	F	34	165	60	3,400
6	F	22	160	51	3,400
7	F	31	175	58	3,000
8	F	27	168	66	3,900
Mean $\pm$ SD		$35 \pm 10$	$171 \pm 7$	$67 \pm 12$	$3,800 \pm 650$

MEV, maximum exhaled volume; M, male; F, female.

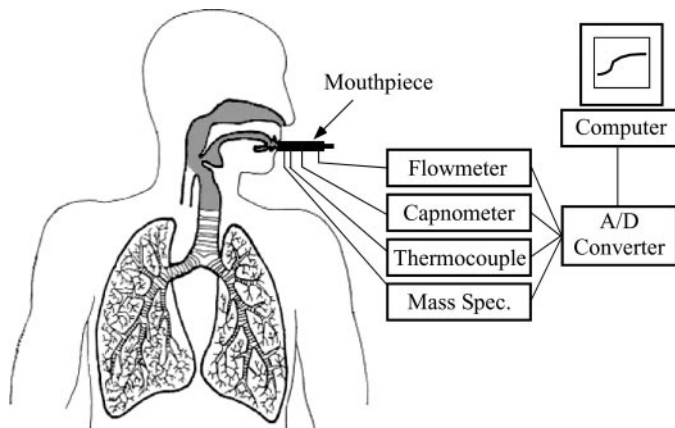


Fig. 1. Schematic of experimental setup. A linear resistance attached to the end of the mouthpiece and a display of their exhaled flow rate on the computer monitor helped subjects maintain a constant exhaled flow rate. Acetone concentration was measured by using the mass spectrometer. A/D, analog to digital.

(CO<sub>2</sub>SMO, Novamatrix Medical Systems, Wallingford, CT), and a linear resistance that was manually changed, depending on the desired exhaled flow rate. The signals from all four instruments were converted from analog to digital, sampled at 20 Hz, and displayed on the monitor of a Macintosh 7100 computer running Chart (AD Instruments, Mountain View, CA). Figure 1 displays a diagram of this setup.

**Isothermal rebreathing device.** The isothermal rebreathing device, similar to that described by Ohlsson et al. (29) and Martin (22), consisted of a 10-liter Mylar bag and heating pad placed inside a Styrofoam box. The temperature inside the box was measured with a thermocouple, maintained between 37 and 40°C throughout the experiment, and controlled electronically by turning the heating pad on or off. A side hole in the Styrofoam box allowed the Mylar bag to be connected via a small segment of tubing to an external mouthpiece and pneumotach. Initially, the Mylar bag contained 2 liters of warm (temperature > 37°C) ambient air. Once a rebreathing maneuver was completed, the rebreathed air was sampled with a warm gastight syringe.

**Protocol.** The design of this experiment focused on measuring two quantities: 1) the partial pressure of endogenous acetone in the alveolar air using an isothermal rebreathing maneuver; and 2) the partial pressure of endogenous acetone in the exhaled breath throughout a prolonged exhalation maneuver. At the start of the experiment, subjects were asked to perform the rebreathing maneuver in triplicate. For a single rebreathing maneuver, a seated subject donned a nose clip and placed his or her mouth on the mouthpiece connected to the rebreathing device. The subject then inhaled between 1 and 1.5 liters of air from the Mylar bag in the rebreathing device, exhaled back into the Mylar bag, and repeated this maneuver seven more times for a total of eight breaths. At the completion of the rebreathing maneuver (i.e., the end of the eighth exhalation), the tubing was clamped, the mouthpiece and pneumotach were removed from the tubing, and a warm (temperature > 50°C) gastight syringe with a three-way stopcock was connected. Two hundred milliliters of air were removed from the Mylar bag before 50 ml of rebreathed air were sampled and subsequently analyzed with the mass spectrometer. Once three rebreathing maneuvers were completed, each subject performed two different prolonged maneuvers, with each set repeated three times. For both maneuvers, the subject donned nose clips and inhaled quickly from functional residual capacity (FRC) to TLC, placed his or her lips on the mouthpiece, and exhaled at a constant rate. The subject's exhaled flow rate and the target exhaled flow rate were displayed on a computer monitor, whereby the subject could adjust his or her

exhalation rate, if necessary, to match the target flow rate. The maneuvers differed in the speed of the constant exhalation: *maneuver A* was a slow exhalation (~200 ml/s), and *maneuver B* was a fast exhalation (~350 ml/s). Each maneuver was spaced by 3 min of quiet tidal breathing, during which time the mouthpiece assembly was cooled and dried. The order of the maneuvers was alternated. The protocol described above, including rebreathing and prolonged exhalation maneuvers, was repeated, and then a final set of three rebreathing maneuvers was performed. In total, 9 rebreathing maneuvers and 12 prolonged exhalations (6 slow and 6 fast) were carried out.

To generate a normalized prolonged exhalation profile for each subject and to correct for drift in the mass spectrometer, the raw signal from the mass spectrometer for each of the nine isothermal rebreathing maneuvers was plotted against time for each subject. A best-fit line through all nine rebreathed acetone signals was determined so that an estimate of the mass spectrometer signal for the rebreathed acetone concentration at any point in time could be made. The raw signal generated by the mass spectrometer while measuring acetone during a prolonged exhalation maneuver was normalized by the time-appropriate rebreathing value. Thus a prolonged exhalation profile was produced that was normalized and corrected for drift of the mass spectrometer.

## RESULTS

For each rebreathing maneuver, every subject completed the eight required breaths. The volume of each breath ranged between 1 and 2 liters. Throughout all of the maneuvers, the temperature inside the isothermal rebreathing box was maintained between 37 and 40°C. The concentration of acetone from the isothermal rebreathing maneuvers was plotted against time for each subject (Fig. 2). Each symbol represents the mean and SE of three maneuvers. The slope of the best-fit line through the three data points for each subject was not different from zero ( $P > 0.05$ ).

The maximum exhaled volume of the 12 prolonged exhalation maneuvers performed by each subject is listed in Table 1. The mean exhaled volumes and flow rates for each of the eight subjects are given in Table 2. The flow rate for *maneuver A* was statistically less ( $P < 0.0001$ ) than the flow rate for *maneuver B* for each individual subject and when the data for all eight subjects were combined.

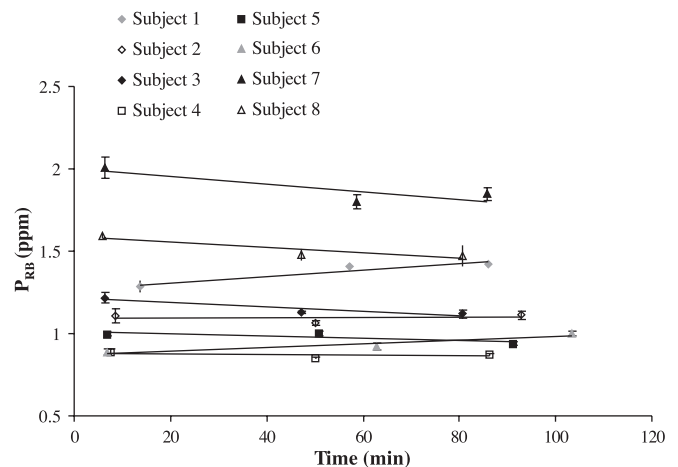


Fig. 2. Isothermal rebreathing concentration vs. time for all eight subjects. Each data point represents the mean  $\pm$  SE of three rebreathing maneuvers. Best fit lines for each subject are presented. The acetone concentration in each of the eight subjects is relatively constant over time. P<sub>REB</sub>, rebreathing partial pressure; ppm, parts per million.

Table 2. Exhaled volumes and flow rates

Subject No.	Maneuver	Exhaled Volume, ml	Flow Rate, ml/s
1	A	4,440±210	202±3
	B	4,350±60	346±6
2	A	4,480±130	194±3
	B	4,300±110	337±8
3	A	2,810±180	194±5
	B	2,900±160	338±13
4	A	3,850±90	193±2
	B	3,820±70	348±5
5	A	3,160±90	215±7
	B	3,150±50	369±15
6	A	2,930±150	177±5
	B	3,210±80	317±12
7	A	2,540±220	213±11
	B	2,630±220	338±15
8	A	3,680±30	190±9
	B	3,650±40	333±16
Mean±SD	A	3,490±740	197±12
	B	3,500±630	341±15

A simple smoothing algorithm (a 10-point moving average filter) removed high-frequency noise from each normalized acetone profile. The resulting profiles have three distinct phases (Fig. 3). Phase I represents the initial volume of air that does not contain acetone. Phase II is the transition from dead space to exchange space, and phase III represents the dynamics of the exchange space. For acetone and other highly soluble gases, the air in the conducting airways contains acetone and, therefore, is considered part of the exchange space. Phase I, not present in Fig. 3, represents dead space volume that delays the appearance of acetone at the mouth. For exhaled acetone, this volume consisted only of instrument dead space (i.e., no physiological dead space), which was subtracted from the profiles before presentation in Fig. 3. Next, each trial was truncated to the smallest exhaled volume for a given subject. For example, because the smallest exhaled volume within the 12 trials for *subject 2* was 4,170 ml, the data for the remaining 11 trials for *subject 2* were truncated to 4,170 ml. Therefore, differences in exhaled volumes did not confound the analysis. Similar to the study by George et al. (12), each group of profiles within a subject and maneuver type was subsequently condensed into a single representative exhalation maneuver by

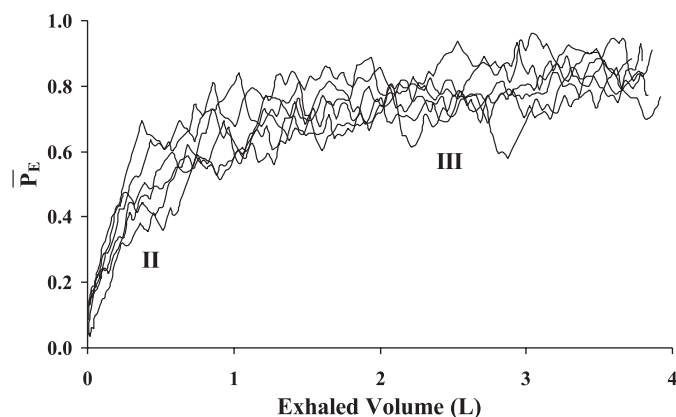


Fig. 3. Six exhalation profiles for *subject 4, maneuver B*. Phases II and III are labeled. The time lag representing instrument dead space has been corrected, thereby eliminating phase I from this plot.  $P_E$ , exhaled acetone normalized by rebreathed acetone partial pressure.

averaging the normalized acetone partial pressure in the exhaled air at intervals of 1/20 of the total exhaled volume (Fig. 4). Condensing the profiles dramatically reduces computer simulation time, as 96 single-exhalation profiles have been reduced to 16, two profiles per subject.

#### Computer Simulations

Before a prolonged breathing maneuver was simulated, the model first must reach breath-to-breath steady-state conditions. The temperature, water concentrations, and acetone concentrations within the mathematical model were brought to steady-state conditions by simulating tidal breathing at FRC. For modeling purposes, we assumed vital capacity was equal to the smallest exhaled volume measured in each subject. A respiratory rate of 12 breaths/min, a sinusoidal flow waveform, and a tidal volume equal to 10% of the vital capacity were used. The inspired air temperature and relative humidity were set to 23°C and 50%, respectively. The partial pressure of acetone in the venous blood entering the pulmonary circulation was set equal to 1 ppm in air. The solubility of acetone in blood ( $\beta_b$ ) and water is a function of temperature. This relationship was estimated based on Wagner et al. (39) and predicts the blood-air and water-air partition coefficients of acetone to be 341 and 279, respectively, at 37°C. The blood-tissue solubility was estimated to be 1.38 (42). Steady-state conditions were reached when the end-exhaled temperature and end-exhaled acetone concentration changed by <0.1% between breaths. Then the model simulated a single-exhalation maneuver performed at three-fourths of TLC. Each prolonged exhalation was preceded by a single inhalation from FRC to TLC. This volume (inspiratory reserve volume + tidal volume) was approximated as 75% of the vital capacity (15), with the assumption that each subject inhaled to TLC. The expired volume was specified to be the minimum expired volume used to condense the profiles of each subject. Additionally, the exhalation time must be specified to simulate each condensed exhalation maneuver. The exhalation time was determined by dividing the expired volume by the mean flow rate for the group of maneuvers corresponding to the condensed profile.

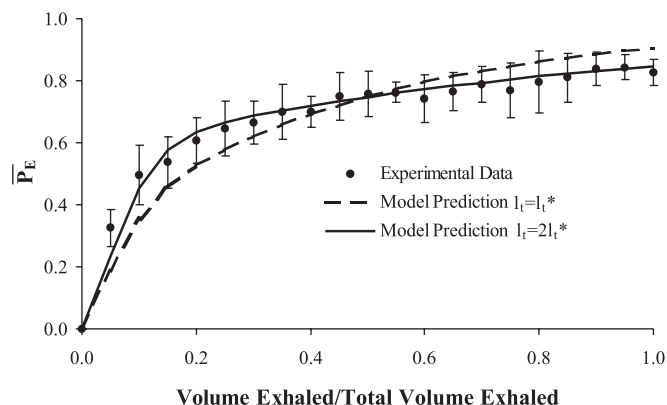


Fig. 4. Condensed exhalation profile (●) for *subject 4, maneuver B*, is shown with predictions from the mathematical model using two values for the connective tissue thickness ( $l_t$ ): the value from Anderson et al. (1) (dashed line;  $l_t^*$ ) and twice the value of Anderson (solid line;  $2l_t^*$ ). Doubling the  $l_t$  dramatically improves the predicted exhalation profile. Each point in the condensed profile represents the mean of the six corresponding points in Fig. 3 at increments of 1/20 of the normalized exhaled volume. Values are means ± SD.

Across maneuver type and subject, three distinct differences were apparent between the model's predictions and the experimental data (Fig. 4). Compared with the data, the model predicted: 1) a smaller rise in acetone concentration during phase II; 2) a larger phase III slope ( $S_{III}$ ), as calculated from a best-fit line through the interval from 50 to 90% of exhaled volume; and 3) a larger acetone partial pressure in the end-exhaled air normalized to the rebreathed partial pressure ( $\bar{P}_{E_{end}}$ ). By doubling the thickness of the connective tissue layer (Fig. 4) and maintaining constant the thickness of the airway wall (airway wall = connective + adventitial tissue), model predictions were improved dramatically as measured by the correlation coefficient,  $R^2$ , between the model prediction and the condensed profile. The  $S_{III}$  (mmHg acetone in air · mmHg acetone in rebreathed air<sup>-1</sup> · l<sup>-1</sup>) and  $\bar{P}_{E_{end}}$  for both the condensed profiles and the profiles predicted by the model using a doubled connective tissue layer are summarized in Table 3 with the associated  $R^2$ . Statistical comparisons between experimental or model  $S_{III}$ ,  $\bar{P}_{E_{end}}$ , or end-exhaled temperature were made using a paired two-sided  $t$ -test.  $S_{III}$  is statistically different from zero ( $P < 0.05$ ) for all  $S_{III}$ , except for two slow experimental maneuvers. No statistical difference exists within a subject between slow and fast maneuvers for experimentally measured  $S_{III}$ . The mean experimental  $S_{III}$  values for *maneuvers A* and *B* are not statistically different. The mean of all  $S_{III}$  values from the condensed profiles is  $0.054 \pm 0.016$  mmHg acetone in air · mmHg acetone in rebreathed air<sup>-1</sup> · l<sup>-1</sup> and is statistically different from the mean of the model-predicted  $S_{III}$ . The mean model-predicted  $S_{III}$  values for *maneuvers A* and *B* are statistically different. However, this difference appears to be an artifact of fitting the model to the data. When the two simulations that do not accurately predict the data (i.e.,  $R^2 < 0.9$  for *subjects 6A* and *7A*) are removed from the statistical analysis, the model-predicted  $S_{III}$  values for *maneuvers A* and *B* are not statistically different. Four of the eight subjects had statistically different values of  $\bar{P}_{E_{end}}$  between *maneuvers A* and *B*. As a result,  $\bar{P}_{E_{end}}$  between *maneu-*

*vers A* and *B* for all subjects is statistically different between *maneuvers A* and *B* for both experimental and predicted profiles. The mean of all experimentally measured  $\bar{P}_{E_{end}}$  is  $0.82 \pm 0.05$  and is statistically different from the model-predicted mean value. For both  $S_{III}$  and  $\bar{P}_{E_{end}}$ , the model fit *maneuver B* better than *A*. By doubling the thickness of the connective tissue layer, the accuracy of the model-predicted experimental profiles increase from an  $R^2 = 0.78$  to an  $R^2 = 0.94$ . The measured end-exhaled temperature was not statistically different between *maneuvers A* and *B* for subjects individually and as a group. The mean end-exhaled temperature across all subjects and maneuvers was  $34.1 \pm 0.7^\circ\text{C}$  and is not statistically different from the mean model-predicted end-exhaled temperature across all subject and maneuvers of  $34.2 \pm 0.2^\circ\text{C}$  when the connective tissue thickness ( $l_t$ ) =  $2l_t^*$ , where  $2l_t^*$  is  $l_t$  that is twice that used in Anderson et al. (1).

The model has been used previously to determine location of acetone exchange in the lung (1). Simulations of tidal breathing predicted that >95% of acetone exchange occurs within the airways, whereas <5% of exchange occurs in the alveoli. Before similar model predictions for a prolonged exhalation are examined, it is helpful to briefly describe the mechanisms of airway gas exchange. As fresh air is inspired, this air absorbs acetone from the mucous layer, thereby depleting the acetone concentration in the airway wall. Because of the small bronchial blood flow ( $\dot{Q}_{br}$ ) and the significant tissue barrier between the bronchial circulation and mucus layer, the mucus is not replenished with acetone before expiration begins. During expiration, the air encounters a lower concentration of acetone in the mucus and, therefore, a large driving force for the deposition of soluble gas onto the mucus. This large air-to-mucus gradient promotes recovery of acetone by the mucous layer and delays the rise in acetone concentration at the mouth, thus accounting for the  $S_{III}$ . These absorption-desorption phenomena decrease the amount of soluble gas leaving the lung late in exhalation and are the major mechanisms of pulmonary

Table 3. Phase III ( $S_{III}$ ),  $\bar{P}_{E_{end}}$ , and  $R^2$

Subject No.	Maneuver	$S_{III}$ (Data)	$S_{III}$ (Model, $2l_t^*$ )	$\bar{P}_{E_{end}}$ (Data)	$\bar{P}_{E_{end}}$ (Model, $2l_t^*$ )	$R^2$ ( $l_t = l_t^*$ )	$R^2$ ( $l_t = 2l_t^*$ )
1	A	0.039	0.064	0.80	0.86	0.70	0.94
	B	0.034	0.051	0.80	0.84	0.88	0.98
2	A	0.039*	0.065	0.81	0.86	0.83	0.97
	B	0.045	0.052	0.85	0.85	0.93	0.98
3	A	0.069	0.096	0.79	0.84	0.67	0.92
	B	0.083	0.074	0.84	0.83	0.74	0.93
4	A	0.043	0.072	0.78†	0.87	0.72	0.93
	B	0.051	0.056	0.83	0.85	0.88	0.98
5	A	0.079	0.082	0.85†	0.86	0.92	0.99
	B	0.060	0.064	0.92	0.84	0.91	0.94
6	A	0.058	0.096	0.70†	0.85	0.44	0.81
	B	0.070	0.074	0.81	0.83	0.77	0.96
7	A	0.045*	0.103	0.81	0.83	0.64	0.84
	B	0.036	0.081	0.86	0.82	0.74	0.91
8	A	0.073	0.074	0.79†	0.87	0.81	0.96
	B	0.041	0.059	0.87	0.85	0.91	0.99
Mean ± SD	A	0.056 ± 0.016	0.082 ± 0.015†	0.79 ± 0.04†	0.85 ± 0.01†	0.72 ± 0.15†	0.92 ± 0.06
	B	0.053 ± 0.017	0.064 ± 0.011	0.85 ± 0.04	0.84 ± 0.01	0.85 ± 0.08	0.96 ± 0.03
	A and B	0.054 ± 0.016	0.073 ± 0.016	0.82 ± 0.05	0.85 ± 0.01	0.78 ± 0.13	0.94 ± 0.05

$S_{III}$ , slope of phase III (mmHg acetone in air · mmHg acetone in rebreathed air<sup>-1</sup> · l<sup>-1</sup>);  $\bar{P}_{E_{end}}$ , normalized partial pressure of acetone in exhaled air at end expiration;  $l_t$ , connective tissue thickness;  $l_t^*$ ,  $l_t$  based on Anderson et al. (1);  $2l_t^*$ ,  $l_t$  twice that of Anderson et al. \*Not statistically different from 0 ( $P < 0.05$ ); †Statistical difference between *maneuvers A* and *B* ( $P < 0.05$ ).

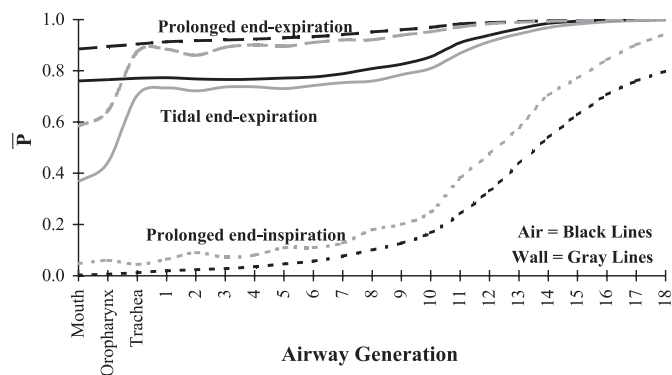


Fig. 5. Axial profiles of acetone partial pressure ( $\bar{P}$ ) in the airway (black lines) and airway wall (gray lines) normalized to alveolar partial pressure, as calculated from the mathematical model. Relative to the axial profile for the end expiration of a tidal breath (solid line), the axial profile at end inspiration of a prolonged inspiration to total lung capacity (short dashed line) is dramatically reduced, whereas the axial profile at end expiration of a prolonged exhalation maneuver (long dashed line) is increased. The relationship between these axial profiles is a major factor determining the airway fluxes presented in Fig. 6.

gas exchange for acetone and any gas with a blood-air partition coefficient ( $\lambda_b$ )  $>100$  (1).

To examine these absorption-desorption phenomena during a single-exhalation maneuver, the molar flow of acetone from the airway wall to the airway lumen for a given time period (e.g., inspiration) and airway generation can be calculated by expressions described previously (1). The distribution of acetone flow to and from the airway wall per airway generation was studied by simulating the exchange of acetone in an average lung. The parameters used in these simulations were based on the mean vital capacity and flow rate for *maneuvers A* and *B* of the eight subjects. Additionally, the effect of changing mucous layer thickness from  $l_t^*$  to  $2l_t^*$  was studied, where  $l_t^*$  is  $l_t$  based on Anderson et al.

To calculate the molar flows of acetone (mol/s) from the airway wall to the airway lumen, the axial profile of acetone partial pressure within the airway lumen and airway wall must be known at multiple time points throughout a breath. The solution of the mathematical model yields the axial profile of partial pressure within the airway lumen and airway wall (and all other layers as well) for any desired time during inspiration and expiration. Figure 5 shows axial profiles of acetone partial pressure at end expiration of a normal tidal breath, followed by end inspiration and end expiration of a prolonged maneuver. At end expiration of a tidal breath, the partial pressure of acetone for all airway generations is greater in the airway lumen ( $P_{air}$ ) than the airway wall ( $P_{wall}$ ) (solid black and solid gray lines, respectively). If the next breath is a large prolonged inspiration (small dashed line) from FRC to TLC, fresh air will enter the lungs and cause  $P_{air}$  at the mouth, oropharynx, and trachea to be approximately zero. After the airways have been replaced with fresh air,  $P_{wall} - P_{air}$  is always greater than zero during inspiration. This difference decreases throughout inspiration (not shown), as acetone is stripped from the wall by the inspired air that is void of acetone at the mouth. On expiration, alveolar air with  $P_{air} = 1.0$  begins its passage through the airways to exit at the mouth. Because the air entering the airways at generation 18 has  $P_{air} = 1.0$ , the difference,  $P_{wall} - P_{air}$ , is less than zero for the final 90% of the prolonged

exhalation. At each generation, it is this driving force,  $P_{wall} - P_{air}$ , that causes acetone to reabsorb back onto the airway wall throughout expiration and causes the fluxes of acetone shown in Fig. 6. Interestingly, the axial profile of acetone partial pressure is greater at end expiration for a prolonged maneuver than a tidal breath, because the volume of air passing through the airways during inhalation and exhalation with  $P_{air} = 1.0$  is 10-fold greater during a prolonged exhalation than a tidal exhalation.

From these axial profiles of acetone partial pressure (Fig. 5), the flow of acetone (mol/s) from the airway wall to the airway

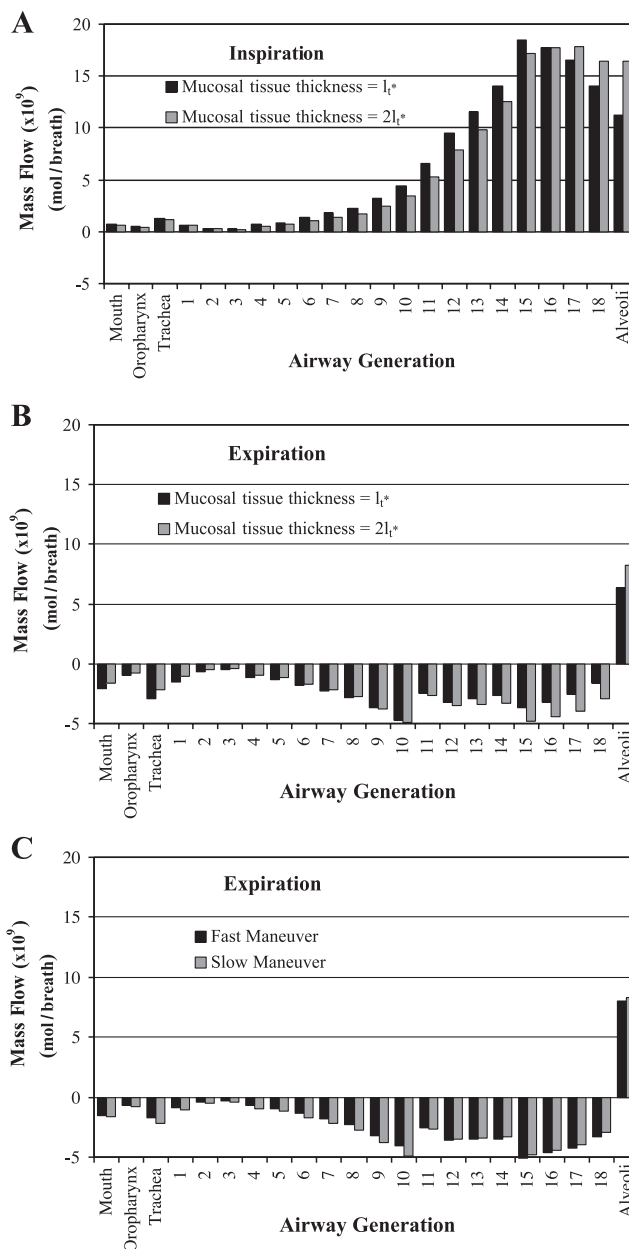


Fig. 6. Axial distribution of acetone transport during inspiration (A) and expiration (B) for a slow-exhalation maneuver. Solid bars indicate a model lung with a  $l_t$  described by Anderson et al. (1),  $l_t^*$ , and the shaded bars indicate a model lung with a  $l_t = 2l_t^*$ . C: axial distribution of acetone transport during a slow (shaded) and fast (solid) exhalation for  $l_t = 2l_t^*$ . Positive flow denotes tissue to air; negative denotes air to tissue.

lumen for a given axial position (e.g., the trachea) and period of time can be calculated and is dependent on the difference in acetone partial pressure between the wall and lumen,  $P_{\text{wall}} - P_{\text{air}}$ , multiplied by the mass transfer coefficient, which is a function of air-stream velocity. For a given axial position, such as an airway generation, these flows or fluxes of acetone can be summed together over all time points throughout an inspiration and/or expiration. The sum of these fluxes from airway wall to lumen over an inspiration for each airway generation is plotted in Fig. 6 and represents the axial distribution of acetone transport from the airway wall to the lumen (positive flux). The transport of acetone per generation during inspiration (Fig. 6A) and expiration (Fig. 6B) is presented for two cases during a slow, prolonged exhalation: 1)  $l_t^*$  and 2)  $2l_t^*$ .

On inspiration (Fig. 6A), the axial distribution of acetone fluxes is bimodal. Independent of the connective tissue thickness, a small peak occurs in the trachea. A larger peak is present at the 15th generation and shifts to the 17th generation when  $l_t$  doubles. Independent of  $l_t$ , this peak results from an increase in surface area, decrease in connective tissue layer thickness, and increase in  $\dot{Q}_{\text{br}}$  relative to the mean as the airways progressively bifurcate. Doubling  $l_t^*$  causes an increased diffusional resistance to acetone transport from the bronchial circulation to the airway lumen. Thus the acetone flux distribution shifts to smaller airways with thinner airway walls (airway wall thickness = connective tissue + adventitial tissue thickness) that permit the pulmonary circulation to play a significant role in acetone exchange with the air in the airway lumen. Additionally, the model predicts that alveolar gas exchange plays a larger role in acetone exchange when the connective tissue thickness is increased.

On expiration (Fig. 6B), the gas in the alveoli continues to pick up acetone from the pulmonary circulation. The axial distribution of acetone fluxes is trimodal. As the air saturated with acetone leaves the alveoli and enters the airways, the air loses acetone to the mucous surface. This loss reaches a peak at *generation 15* and serves to offset the large positive flux over these last generations seen during inspiration. Another peak is present at *generation 10* and results from a 10-fold reduction in the molecular diffusion coefficient in the adventitial layer to account for the appearance of cartilage in *generations 1–10*. In these generations, the partial pressure of acetone is reduced compared with airway generations  $>10$ , because only the bronchial circulation replenishes the mucous layer with acetone, whereas, in generations  $>10$ , both the pulmonary and bronchial circulations participate in recharging the mucous layer. This reduction in acetone concentration increases the driving force for recovery of acetone that results in the peak at *generation 10*. In the trachea, a peak is present that is more negative than its corresponding flux during inspiration is positive. Therefore, more acetone is deposited into the tracheal mucosa during expiration than was absorbed into the air-stream during inspiration, which accounts for an upwards shift in the axial profile of acetone between end-exhalation of a tidal breath and of a prolonged maneuver (Fig. 5). Figure 6B demonstrates that a doubling of  $l_t^*$  causes the acetone fluxes in the first 8 generations to be reduced and the fluxes in generations  $>8$  to be enhanced relative to the lung with  $l_t = l_t^*$ . Practically, this shifts the burden of acetone gas exchange during expiration to the smaller airways and alveoli. However, this shift in location of gas exchange does not affect the

fraction of acetone recovered by the airways during exhalation. Of the acetone transferred from the mucous layer to the respired air, 35% is desorbed onto the airways during expiration. Interestingly, this fraction is independent of the connective tissue thickness. During a prolonged breathing maneuver, airway gas exchange accounts for 81% of acetone exchange in the lungs when  $l_t = l_t^*$  and 73% when  $l_t = 2l_t^*$ . This percentage is based on the net (inspiration + expiration) airway gas transport normalized by net airway and alveolar gas transport.

To examine the effects of exhaled flow rate on the axial distribution of acetone flux, only the axial fluxes during exhalation need to be examined, as the inspired rate was assumed to be constant, irrespective of exhalation maneuver. Figure 6C shows the axial distribution of acetone fluxes over a slow and fast maneuver for a lung with  $l_t = 2l_t^*$ . Figure 6C demonstrates that an increase in exhaled flow rate causes an increase in the acetone flux in the airway generations nearest the alveoli, *generations 13–18*, and a decrease in acetone flux from the mouth to *generation 10*. The reason *generations 13–18* have larger acetone fluxes over a fast exhalation than a slow exhalation can be understood by examining acetone transport in *generation 18*. Over the entire expiration, the partial pressure of acetone entering *generation 18* is alveolar (i.e., equal to the partial pressure in blood) and is independent of exhalation rate. Thus the only mechanism to increase flux is to increase the mass transfer coefficient, which increases as a function of flow rate. This mechanism is more important than residence time for the six generations nearest the alveoli.

The mathematical model is able to better predict the experimental data by using an increased connective tissue layer thickness that is twice the value used in Anderson et al. (1). In addition, the model predicts that the majority of acetone exchange occurs within the conducting airways and not the alveoli. The interaction of acetone with the airways can subsequently be used to explain the shape of the exhalation profile.

## DISCUSSION

### Mass Spectrometer

Hundreds of compounds have been identified in the exhaled breath of humans (30, 32). Many of these compounds in the exhaled breath are exogenous in origin. With examination of endogenous gases in the exhalate (excluding respiratory gases), acetone is present at levels that are at least 4- to 10-fold greater than most currently detectable endogenous gases found in normal humans (5, 8, 25). Nevertheless, we verified that the mass spectrometer was solely detecting acetone. To examine whether acetone was present in the ambient air, the mass spectrometer sampled both 100%  $O_2$  and room air. The peak at a mass-to-charge ratio of 58 did not change between the two test gases. Additionally, we measured a few of the isothermal rebreathing samples with both our mass spectrometer and a gas chromatograph (Hewlett-Packard Series II 5890 GC, Santa Clara, CA). We found the acetone measurements made with the mass spectrometer were tightly correlated to the same measurements performed with the gas chromatograph. These results were expected because the gases most likely to interfere with the acetone measurements would be either small chain ketones or aldehydes. However, most of these species were not observed in the exhaled breath or, if observed, did not have a peak at a mass-to-charge ratio = 58. For example, propanal

(i.e., propionaldehyde) also has a large peak at a mass-to-charge ratio = 58. However, Phillips et al. (32) used gas chromatography to analyze volatile organic compounds in the exhaled breath and did not detect propanal. Methyl phenyl ketone was observed in 94% of the subjects in Phillips et al. However, the mass spectrum of this ketone does not have a peak at a mass-to-charge ratio = 58 and, most likely, is present at 10-fold smaller concentrations than acetone in the breath. Thus it should not confound our measurements of acetone.

### *Isothermal Rebreathing*

Isothermal rebreathing is used in this study because it allowed noninvasive sampling of acetone in the alveolar air (i.e., air in equilibrium with blood). Consequently, a venous blood sample was unnecessary. Rebreathing assists the equilibration of air in the lung with the pulmonary blood by closing the respiratory circuit, maintaining a single mass of air in close contact with the blood for 30–45 s, and mixing the air by inspiration and expiration. Because acetone is very water soluble and its solubility is inversely related to temperature, the temperature of the rebreathing system was maintained between 37 and 40°C to reduce condensation of acetone onto the airway walls as a result of cooling and, therefore, to reduce the time to equilibration. Isothermal rebreathing has been used in multiple studies to provide a more faithful representation of alveolar gas (18, 22, 29). Two of these studies demonstrated that ethanol concentrations recovered from isothermal rebreathing maneuvers are an accurate representation of the blood alcohol level in human subjects. The data from Jones (18) and Ohlsson et al. (29) demonstrated that breath samples from isothermal rebreathing were within  $\pm 10\%$  of the blood alcohol levels after five and six breaths, respectively. Jones (18) demonstrated that increasing the number of rebreathing breaths produced higher breath alcohol concentrations than the single-exhalation maneuver and that most of the change in rebreathed alcohol concentration occurred within the first three rebreathing breaths. Recently, Martin (22) used isothermal rebreathing to evaluate three methods (mixed exhaled, end exhaled after a breath hold, and rebreathing) used to collect samples of alveolar air for a series of gases. The blood solubility of these gases ranged over three orders of magnitude from halothane to ethanol, with acetone residing in the middle. Martin found that rebreathing provided the closest estimate of blood concentration as measured by a blood solubility parameter, the  $\lambda_b$ . The rebreathing protocol used in this study resembled the procedure used by Martin (22) and required moderate respired volumes (1–2 liters) and eight or more breathing cycles. Based on our observations, isothermal rebreathing appeared to produce a repeatable measurement of alveolar air that was consistent with the observations of those previous studies.

### *End Exhaled Is Not Alveolar Air*

Our experimental data demonstrate that the acetone in end-exhaled air is  $\sim 80\%$  of the acetone partial pressure in the corresponding rebreathing sample. The end-exhaled partial pressure depends statistically ( $P < 0.05$ ) on the rate of the constant exhalation. For a slow exhalation,  $\bar{P}_{E_{\text{end}}} = 0.79 \pm 0.04$  and for a fast exhalation,  $\bar{P}_{E_{\text{end}}} = 0.85 \pm 0.04$ . The model did not predict this dependence of  $\bar{P}_{E_{\text{end}}}$  on exhaled flow rate. From the modeling study presented here, it is difficult to

determine the physiological parameters that underlie the relationship between  $\bar{P}_{E_{\text{end}}}$  and exhaled flow rate. A few studies have speculated that the uncertainty in this model's predictions results from uncertainty concerning the mass transfer coefficient, because the correlations describing the mass transfer coefficients break down at low Reynolds numbers (i.e., small flow rates), which occur in the small airways (3, 7). While those studies have explored this issue for ethanol, water, and nitric oxide, the effect of the mass transfer coefficient, specifically, or most model parameters, in general, on acetone exchange in the airways is not clearly understood. In the future, these relationships may be revealed by submitting the mathematical model to a sensitivity analysis. Because  $\bar{P}_{E_{\text{end}}}$  depends on the exhaled flow rate, studies measuring endogenous acetone in the breath will need to control this parameter. We were unable to find a single study measuring exhaled endogenous acetone that controlled exhaled flow rate during the collection or sampling of the air. Controlling exhaled flow rate may provide a more consistent measurement and facilitate more accurate comparisons between different subject populations and laboratories.

While the dependence of  $\bar{P}_{E_{\text{end}}}$  on flow rate is interesting, the fact that  $\bar{P}_{E_{\text{end}}}$  is not equal to 1.0 (i.e., rebreathed air) is more important. Most studies measuring endogenous acetone assume that the end-exhaled air is alveolar air (10, 21, 25, 27, 36). Based on our study and assuming that rebreathed air is alveolar air, most studies appear to underestimate alveolar air by  $\sim 20\%$ , if they use a prolonged exhalation, and by  $\sim 30\%$ , if they use a tidal breath [see  $\bar{P}_{\text{air}}$  at mouth in Fig. 5 and Anderson et al. (1)]. As stated above, this variation makes comparisons between different subject populations or laboratories less accurate. Of the maneuvers used in this study, isothermal rebreathing appeared to provide a more consistent and representative measure of alveolar air than the prolonged exhalation maneuver.

### *Airway Exchange of Acetone*

Gas exchange in the lung can occur in the alveoli and/or the airways. Gases that exchange exclusively in the alveoli, such as SF<sub>6</sub>, ethane, and carbon dioxide, have  $\lambda_b < 10$ . Theoretical predictions show that gases with  $\lambda_b > 100$ , such as acetone, isopropanol, and ethanol, exchange exclusively in the airways (1). Gases with  $\lambda_b$  between 10 and 100 exchange in both spaces. Experimentally, the interaction of acetone with the airways has been recognized for  $>40$  yr. An early study of soluble gas exchange by Cander and Forster (4) demonstrated unusually high end-tidal concentrations of diethyl ether ( $\lambda_b \approx 15$ ) and acetone ( $\lambda_b \approx 340$ ) during washin of these gases. These authors concluded that inspired soluble gases were dissolved in the tissues of the respiratory dead space during inspiration and revaporized during expiration. A similar conclusion was reached by Wigaeus et al. (41) in their studies of the uptake and elimination of acetone. Schrikker et al. (34, 35) carried out a more detailed evaluation of airway interaction. These authors performed short-duration washin and washout experiments with the soluble gases diethyl ether ( $\lambda_b \approx 15$ ), ethyl acetate ( $\lambda_b \approx 75$ ), and acetone ( $\lambda_b \approx 340$ ). The excretions ( $PE/P\bar{v}$ , where PE is mixed-exhaled partial pressure and  $P\bar{v}$  is mixed-venous partial pressure) values for acetone (the highest solubility) were lowest of the three, an observation that

is inconsistent with simple alveolar gas exchange from parallel compartments (9). Analysis of the gas tension at the mouth during a single exhalation showed that, for acetone, the volume of gas expired before the beginning of phase II (the rapid rise phase of the exhaled inert-gas partial pressure profile, e.g., during N<sub>2</sub> washout), a volume considered to represent anatomic dead space, was considerably smaller than that found for ether. Similarly, the present study found that phase I was not detectable in any of the acetone prolonged exhalations. This observation is consistent with airway interaction of the more soluble gas, acetone. Their second study (34) used a washin method to quantify the excretion values for four soluble gases: ethyl acetate ( $\lambda_b \approx 75$ ), acetone ( $\lambda_b \approx 340$ ), ethanol ( $\lambda_b \approx 2,000$ ), and acetic acid ( $\lambda_b \approx 20,000$ ). With the use of even more soluble gases than in the earlier study, it was shown that the excretion values were lower for the more soluble gases, an observation consistent with a substantial interaction of respired gas with the airway epithelial tissue. During inhalation, gases evaporate from the airway surface and are inspired. During exhalation, the soluble gases are lost from the exhalate onto the airway surface. The relative elimination of the gas is thus decreased due to airway interaction.

### Model Predictions

To fit the mathematical model to the experimental data, three of the model predictions needed to be adjusted (Fig. 4) as follows: 1) increasing the phase II slope; 2) decreasing the  $S_{III}$ ; and 3) decreasing  $P_{E_{end}}$ . Based on our experience with this mathematical model (1, 12) and our understanding of airway gas exchange (33, 37, 38), a variety of parameters describing tissue diffusion and perfusion were adjusted ad hoc to increase the predictive accuracy of the model. The following parameters were independently doubled and halved to examine their effects on the three model outputs: 1) tissue diffusion parameters: molecular diffusivity of acetone through tissue ( $D_t$ ), capillary surface area ( $A_s$ ), solubility of acetone in tissue ( $\beta_t$ ), and the  $l_t$ ; and 2) bronchial perfusion parameters:  $\dot{Q}_{br}$ , and capillary cross-sectional area. Most parameters slightly affected one or perhaps two of the model outputs, phase III or  $P_{E_{end}}$ . Only doubling the connective tissue layer notably changed all three model outputs in the desired direction. We are uncertain that doubling the connective tissue layer from the value used in Anderson et al. (1) (120  $\mu\text{m}$  in the trachea to 28  $\mu\text{m}$  in the 18th generation) is realistic. The connective tissue layer thickness and capillary surface area were calculated using allometric scaling of measurements made in sheep to those in humans (1, 2). Additionally, other studies (3, 13) have assumed values that are similar to the values calculated in Anderson et al. (1) for the corresponding layer in their mathematical models. Consequently, we believe this adjustment in  $l_t$  indicates that the diffusing capacity needs to be refined to appropriately account for acetone exchange. Diffusing capacity ( $D_L$ ) for the airway tissue can be defined.

$$D_L = \frac{D_t \beta_t A_s}{l_t}$$

Based on the measurements of ethanol diffusion through airway tissue (11), we know that  $D_t = 0.33 D_w$  for ethanol, where  $D_w$  is the molecular diffusivity of solute through water. For acetone, this relationship may change slightly. Compared with

ethanol, acetone is a slightly larger molecule, which may reduce  $D_t$ , but the ratio of oil solubility to water solubility is fivefold larger for acetone (24), which may allow it to diffuse more readily through a largely lipid tissue layer (13). The solubility of acetone in tissue ( $\beta_t$ ) used in the simulations was taken from Young and Wagner (42) and is 72% of the solubility of acetone in blood,  $\beta_b$ . Based on their measurements,  $\beta_t$  can range from 50 to 100% of  $\beta_b$ . Evaluating the effect of every possible parameter on the mathematical model's prediction of acetone exchange is cumbersome, unless done properly with a sensitivity analysis (3). A sensitivity analysis in combination with a model validation using ethanol data (12) and acetone data could address this issue.

In conclusion, we measured endogenous acetone in the exhaled breath to evaluate acetone exchange in the lung and found: 1) phase I representing dead space air was not detected; 2) the  $S_{III}$  was positive and was independent of flow rate; 3) normalized end-exhaled acetone concentration was dependent on flow rate; and 4) the majority of acetone exchange occurs in the airways of the lung. In light of these findings, assays using exhaled acetone measurements may need to be reevaluated because they could be underestimating acetone levels in the blood. The most widely used method for collecting endogenous acetone in the exhaled breath makes two critical assumptions. Most investigators discarded the first portion of the breath, assuming that it is "dead-space air" that has not contributed to gas exchange, and sample the final part of the exhalation because it represents alveolar air. This study demonstrates that dead-space air does not exist for acetone, as the airways participate in acetone exchange. Additionally, end-exhaled breath underestimates alveolar air by  $\sim 20\%$  when sampling a prolonged exhalation and by more (perhaps 30%) when sampling a tidal breath. These data suggest that isothermal rebreathing may provide a more representative "alveolar gas" sample than a single-exhaled breathing maneuver when measuring endogenous acetone. Isothermal rebreathing appears to provide a consistent measure of alveolar air, which enables more accurate comparisons between different laboratories, subject populations, species, and experiments.

### ACKNOWLEDGMENTS

We thank Sucheol Gil for assistance with the human subject experiments, Dr. Martin Sadilek for providing time and expertise to fine-tune the mass spectrometer, and Michael S. Morgan for insightful comments and technical advice.

### GRANTS

This work was supported, in part, by National Institute for Biomedical Imaging and Bioengineering Grant T32 EB001650 and by National Heart, Lung, and Blood Institute Grants HL24163 and HL073598.

### REFERENCES

1. Anderson JC, Babb AL, and Hlastala MP. Modeling soluble gas exchange in the airways and alveoli. *Ann Biomed Eng* 31: 1402–1422, 2003.
2. Anderson JC, Bernard SL, Lucht DL, Babb AL, and Hlastala MP. Axial and radial distribution of the bronchial vasculature in sheep. *Respir Physiol Neurobiol* 132: 329–339, 2002.
3. Bui TD, Dabdub D, and George SC. Modeling bronchial circulation with application to soluble gas exchange: description and sensitivity analysis. *J Appl Physiol* 84: 2070–2088, 1998.
4. Cander L and Forster RE. Determination of pulmonary parenchymal tissue volume and pulmonary capillary blood flow in man. *J Appl Physiol* 14: 541–551, 1959.

5. **Capodicasa E, Trovarelli G, De Medio GE, Pelli MA, Lippi G, Verdura C, and Timio M.** Volatile alkanes and increased concentrations of isoprene in exhaled air during hemodialysis. *Nephron* 82: 331–337, 1999.
6. **Chilton TH and Colburn AP.** Mass transfer (absorption) coefficients: prediction from data on heat transfer and fluid friction. *Ind Eng Chem* 26: 1183–1187, 1934.
7. **Condorelli P and George SC.** Theoretical gas phase mass transfer coefficients for endogenous gases in the lungs. *Ann Biomed Eng* 27: 326–339, 1999.
8. **Diskin AM, Spanel P, and Smith D.** Time variation of ammonia, acetone, isoprene and ethanol in breath: a quantitative SIFT-MS study over 30 days. *Physiol Meas* 24: 107–119, 2003.
9. **Farhi LE.** Elimination of inert gas by the lung. *Respir Physiol* 3: 1–11, 1967.
10. **Galassetti PR, Novak B, Nemet D, Rose-Gottron C, Cooper DM, Meinardi S, Newcomb R, Zaldivar F, and Blake DR.** Breath ethanol and acetone as indicators of serum glucose levels: an initial report. *Diabetes Technol Ther* 7: 115–123, 2005.
11. **George SC, Babb AL, Deffebach ME, and Hlastala MP.** Diffusion of nonelectrolytes in the canine trachea: effect of tight junction. *J Appl Physiol* 80: 1687–1695, 1996.
12. **George SC, Babb AL, and Hlastala MP.** Dynamics of soluble gas exchange in the airways. III. Single-exhalation breathing maneuver. *J Appl Physiol* 75: 2439–2449, 1993.
13. **Gerde P and Scott BR.** A model for absorption of low-volatile toxicants by the airway mucosa. *Inhal Toxicol* 13: 903–929, 2001.
14. **Hanna LM and Scherer PW.** Regional control of local airway heat and water vapor losses. *J Appl Physiol* 61: 624–632, 1986.
15. **Hildebrandt J.** Structural and mechanical aspects of respiration. In: *Textbook of Physiology*, edited by Patton HD, Fuchs AF, Hille B, Scher AM, and Steiner R. Philadelphia, PA: Saunders, 1989, p. 991–1011.
16. **Hindmarsh A.** *LSODE*. Livermore, CA: Laurence Livermore Laboratory, 1981.
17. **Ingenito EP.** *Respiratory Fluid Mechanics and Heat Transfer* (PhD thesis). Cambridge, MA: Massachusetts Institute of Technology, 1984.
18. **Jones AW.** Role of rebreathing in determination of the blood-breath ratio of expired ethanol. *J Appl Physiol* 55: 1237–1241, 1983.
19. **Kumagai S and Matsunaga I.** A lung model describing uptake of organic solvents and roles of mucosal blood flow and metabolism in the bronchioles. *Inhal Toxicol* 12: 491–510, 2000.
20. **Kundu SK, Bruzek JA, Nair R, and Judilla AM.** Breath acetone analyzer: diagnostic tool to monitor dietary fat loss. *Clin Chem* 39: 87–92, 1993.
21. **Kupari M, Lommi J, Ventila M, and Karjalainen U.** Breath acetone in congestive heart failure. *Am J Cardiol* 76: 1076–1078, 1995.
22. **Martin MM.** *Comparison of Three Methods of Breath Sampling for Biological Monitoring of Volatile Organic Chemicals*. (PhD thesis). Seattle, WA: University of Washington, 2004.
23. **Mendis S, Sobotka PA, and Euler DE.** Expired hydrocarbons in patients with acute myocardial infarction. *Free Radic Res* 23: 117–122, 1995.
24. **Meulenberg CJ and Vijverberg HP.** Empirical relations predicting human and rat tissue:air partition coefficients of volatile organic compounds. *Toxicol Appl Pharmacol* 165: 206–216, 2000.
25. **Moser B, Bodrogi F, Eibl G, Lechner M, Rieder J, and Lirk P.** Mass spectrometric profile of exhaled breath—field study by PTR-MS. *Respir Physiol Neurobiol* 145: 295–300, 2005.
26. **Musa-Veloso K, Likhodii SS, and Cunnane SC.** Breath acetone is a reliable indicator of ketosis in adults consuming ketogenic meals. *Am J Clin Nutr* 76: 65–70, 2002.
27. **Musa-Veloso K, Rarama E, Comeau F, Curtis R, and Cunnane S.** Epilepsy and the ketogenic diet: assessment of ketosis in children using breath acetone. *Pediatr Res* 52: 443–448, 2002.
28. **Nelson N, Lagesson V, Nosratabadi AR, Ludvigsson J, and Tagesson C.** Exhaled isoprene and acetone in newborn infants and in children with diabetes mellitus. *Pediatr Res* 44: 363–367, 1998.
29. **Ohlsson J, Ralph DD, Mandelkorn MA, Babb AL, and Hlastala MP.** Accurate measurement of blood alcohol concentration with isothermal rebreathing. *J Stud Alcohol* 51: 6–13, 1990.
30. **Pauling L, Robinson AB, Teranishi R, and Cary P.** Quantitative analysis of urine vapor and breath by gas-liquid partition chromatography. *Proc Natl Acad Sci USA* 68: 2374–2376, 1971.
31. **Phillips M, Cataneo RN, Cummin AR, Gagliardi AJ, Gleeson K, Greenberg J, Maxfield RA, and Rom WN.** Detection of lung cancer with volatile markers in the breath. *Chest* 123: 2115–2123, 2003.
32. **Phillips M, Herrera J, Krishnan S, Zain M, Greenberg J, and Cataneo RN.** Variation in volatile organic compounds in the breath of normal humans. *J Chromatogr B Biomed Sci Appl* 729: 75–88, 1999.
33. **Schimmel C, Bernard SL, Anderson JC, Polissar NL, Lakshminarayan S, and Hlastala MP.** Soluble gas exchange in the pulmonary airways of sheep. *J Appl Physiol* 97: 1702–1708, 2004.
34. **Schrikker AC, de Vries WR, Zwart A, and Luijendijk SC.** The excretion of highly soluble gases by the lung in man. *Pflügers Arch* 415: 214–219, 1989.
35. **Schrikker AC, de Vries WR, Zwart A, and Luijendijk SC.** Uptake of highly soluble gases in the epithelium of the conducting airways. *Pflügers Arch* 405: 389–394, 1985.
36. **Smith D, Spanel P, and Davies S.** Trace gases in breath of healthy volunteers when fasting and after a protein-calorie meal: a preliminary study. *J Appl Physiol* 87: 1584–1588, 1999.
37. **Souders JE, George SC, Polissar NL, Swenson ER, and Hlastala MP.** Tracheal gas exchange: perfusion-related differences in inert gas elimination. *J Appl Physiol* 79: 918–928, 1995.
38. **Swenson ER, Robertson HT, Polissar NL, Middaugh ME, and Hlastala MP.** Conducting airway gas exchange: diffusion-related differences in inert gas elimination. *J Appl Physiol* 72: 1581–1588, 1992.
39. **Wagner PD, Naumann PF, and Laravuso RB.** Simultaneous measurement of eight foreign gases in blood by gas chromatography. *J Appl Physiol* 36: 600–605, 1974.
40. **Weibel ER.** *Morphometry of the Human Lung*. New York: Academic, 1963.
41. **Wigaeus E, Holm S, and Astrand I.** Exposure to acetone. Uptake and elimination in man. *Scand J Work Environ Health* 7: 84–94, 1981.
42. **Young IH and Wagner PD.** Solubility of inert gases in homogenates of canine lung tissue. *J Appl Physiol* 46: 1207–1210, 1979.